

OCIP/C 94-7
July 1994

Determination of Leptoquark Properties in Polarized $e\gamma$ Collisions

Michael A. Doncheski and Stephen Godfrey

Ottawa-Carleton Institute for Physics

Department of Physics, Carleton University, Ottawa CANADA, K1S 5B6

We study leptoquark production using polarized $e\gamma$ colliders for the center of mass energies $\sqrt{s} = 500$ GeV and 1 TeV. We show that using polarization asymmetries the ten different types of leptoquarks listed by Buchmüller, Rückl and Wyler can be distinguished from one another for leptoquark masses essentially up to the kinematic limit of the respective colliders. Thus, if a leptoquark were discovered an $e\gamma$ collider could play a crucial role in determining its origins.

PACS numbers: 12.15.Ji, 14.80.Pb, 14.80.Am

There is much interest in the study of leptoquarks (LQs), colour (anti-)triplet, spin 0 or 1 particles, which carry both baryon and lepton quantum numbers. Such objects appear in a large number of extensions of the standard model such as grand unified theories, technicolour, and composite models. Quite generally, the signature for leptoquarks is quite striking: a high p_T lepton balanced by a jet (or missing p_T balanced by a jet, for the νq decay mode, if applicable). Although the discovery of a leptoquark would be dramatic evidence for physics beyond the standard model it would lead to the question of which model the leptoquark originated from. Given the large number of leptoquark types it would be imperative to measure its properties to answer this question.

Following the notation of Buchmüller, Rückl and Wyler (BRW) [1], the complete set of possible LQs numbers 10 is: S_1, \tilde{S}_1 (scalar, iso-singlet); R_2, \tilde{R}_2 (scalar, iso-doublet); S_3 (scalar, iso-triplet); U_1, \tilde{U}_1 (vector, iso-singlet); V_2, \tilde{V}_2 (vector, iso-doublet); U_3 (vector, iso-triplet). The production and corresponding decay signatures are quite similar, though not identical, and have been studied separately by many authors. Even focussing only on the Next Linear Collider (e^+e^- , $e\gamma$ and $\gamma\gamma$ modes), there is a considerable number of works in the literature [2–8]. The question arises as to how to differentiate between the different types. We propose to use a polarized $e\gamma$ collider to differentiate the LQs: a polarized e beam (like SLC) in conjunction with a polarized-laser backscattered photon beam. We concentrate on LQ production in $e\gamma$, which makes use of the fact that the hadronic component of the photon is important and cannot be neglected [5,9,10]. Although the production of LQs in polarized $e\gamma$ collisions was considered first in Ref. [8], those authors do not use the polarization information to determine the specific model of LQ.

We will assume that a peak in the $e + jet$ invariant mass is observed in some collider (*i.e.*, the existence of a LQ has been established), and so we need simply to identify the particular type of LQ. We assume that the leptoquark charge has not been determined and assume no intergenerational couplings. Furthermore, we will assume that only one of the ten possible types of LQs is present. Table 2 of BRW gives information on the couplings to various quark and lepton combinations; the missing (and necessary) bit of information

is that the quark and lepton have the same helicity (RR or LL) for scalar LQ production while they have opposite helicity (RL or LR) for vector LQ production. It is then possible to construct the cross sections for the various helicity combinations and consequently the double spin asymmetry, for the different types of LQs.

We'll denote the various helicity cross sections as $\sigma^{\lambda_e \lambda_q}$, $\lambda_i = +$ for R helicity, $\lambda_i = -$ for L helicity and $\sigma_{TOT} = \sigma^{++} + \sigma^{+-} + \sigma^{-+} + \sigma^{--}$. As is usual in the case of polarized collider phenomenology, it is useful to introduce the double longitudinal spin asymmetry A_{LL} :

$$A_{LL} = \frac{(\sigma^{++} + \sigma^{--}) - (\sigma^{+-} + \sigma^{-+})}{(\sigma^{++} + \sigma^{--}) + (\sigma^{+-} + \sigma^{-+})} \quad (1)$$

and the helicity sum and difference distribution functions of partons within the photon:

$$\begin{aligned} f_{q/\gamma}(x, Q^2) &= f_{q/\gamma}^+(x, Q^2) + f_{q/\gamma}^-(x, Q^2) \\ \Delta f_{q/\gamma}(x, Q^2) &= f_{q/\gamma}^+(x, Q^2) - f_{q/\gamma}^-(x, Q^2) \end{aligned} \quad (2)$$

where $f_{q/\gamma}^{+(-)}(x, Q^2)$ is the probability of a quark with the same (opposite) helicity as the photon to carry a fraction x of the photon's momentum. It is then straightforward to construct A_{LL} for all 10 types of LQs in terms of $\Delta f_{q/\gamma}(x, Q^2) = \Delta f_{\bar{q}/\gamma}(x, Q^2)$, $f_{q/\gamma}(x, Q^2) = f_{\bar{q}/\gamma}(x, Q^2)$ and $\kappa_{L,R}$ ($g_{L,R}^2/4\pi = \kappa_{L,R}\alpha_{em}$). There are 3 general cases:

1) $\sigma^{+\lambda_q} = 0$ (only left-handed electrons couple to LQ):

$$A_{LL}(S_3) = \frac{\int_{M_2/s}^1 dx/x[\Delta f_{u/\gamma}(y, M^2) + 2\Delta f_{d/\gamma}(y, M^2)]f_{\gamma/e}(x)}{\int_{M_2/s}^1 dx/x[f_{u/\gamma}(y, M^2) + 2f_{d/\gamma}(y, M^2)]f_{\gamma/e}(x)} \quad (3)$$

$$A_{LL}(\tilde{V}_2) = -\frac{\int_{M_2/s}^1 dx/x[\Delta f_{u/\gamma}(y, M^2)]f_{\gamma/e}(x)}{\int_{M_2/s}^1 dx/x[f_{u/\gamma}(y, M^2)]f_{\gamma/e}(x)} \quad (4)$$

$$A_{LL}(U_3) = -\frac{\int_{M_2/s}^1 dx/x[\Delta f_{d/\gamma}(y, M^2) + 2\Delta f_{u/\gamma}(y, M^2)]f_{\gamma/e}(x)}{\int_{M_2/s}^1 dx/x[f_{d/\gamma}(y, M^2) + 2f_{u/\gamma}(y, M^2)]f_{\gamma/e}(x)} \quad (5)$$

$$A_{LL}(\tilde{R}_2) = \frac{\int_{M_2/s}^1 dx/x[\Delta f_{d/\gamma}(y, M^2)]f_{\gamma/e}(x)}{\int_{M_2/s}^1 dx/x[f_{d/\gamma}(y, M^2)]f_{\gamma/e}(x)} \quad (6)$$

2) $\sigma^{-\lambda_q} = 0$ (only right-handed electrons couple to LQ):

$$A_{LL}(\tilde{S}_1) = \frac{\int_{M_2/s}^1 dx/x[\Delta f_{d/\gamma}(y, M^2)]f_{\gamma/e}(x)}{\int_{M_2/s}^1 dx/x[f_{d/\gamma}(y, M^2)]f_{\gamma/e}(x)} \quad (7)$$

$$A_{LL}(\tilde{U}_1) = -\frac{\int_{M_2/s}^1 dx/x[\Delta f_{u/\gamma}(y, M^2)]f_{\gamma/e}(x)}{\int_{M_2/s}^1 dx/x[f_{u/\gamma}(y, M^2)]f_{\gamma/e}(x)} \quad (8)$$

3) $\sigma^{-\lambda_q}, \sigma^{+\lambda_\gamma} \neq 0$ (both right- and left-handed electrons couple to LQ):

$$A_{LL}(S_1) = \frac{\int_{M_2/s}^1 dx/x[\Delta f_{u/\gamma}(y, M^2)]f_{\gamma/e}(x)}{\int_{M_2/s}^1 dx/x[f_{u/\gamma}(y, M^2)]f_{\gamma/e}(x)} \quad (9)$$

$$A_{LL}(V_2) = -\frac{\int_{M_2/s}^1 dx/x[\kappa_R(\Delta f_{u/\gamma}(y, M^2) + \Delta f_{d/\gamma}(y, M^2)) + \kappa_L \Delta f_{d/\gamma}(y, M^2)]f_{\gamma/e}(x)}{\int_{M_2/s}^1 dx/x[\kappa_R(f_{u/\gamma}(y, M^2) + f_{d/\gamma}(y, M^2)) + \kappa_L f_{d/\gamma}(y, M^2)]f_{\gamma/e}(x)} \quad (10)$$

$$A_{LL}(U_1) = -\frac{\int_{M_2/s}^1 dx/x[\Delta f_{d/\gamma}(y, M^2)]f_{\gamma/e}(x)}{\int_{M_2/s}^1 dx/x[f_{d/\gamma}(y, M^2)]f_{\gamma/e}(x)} \quad (11)$$

$$A_{LL}(R_2) = \frac{\int_{M_2/s}^1 dx/x[\kappa_R(\Delta f_{u/\gamma}(y, M^2) + \Delta f_{d/\gamma}(y, M^2)) + \kappa_L \Delta f_{u/\gamma}(y, M^2)]f_{\gamma/e}(x)}{\int_{M_2/s}^1 dx/x[\kappa_R(f_{u/\gamma}(y, M^2) + f_{d/\gamma}(y, M^2)) + \kappa_L f_{u/\gamma}(y, M^2)]f_{\gamma/e}(x)} \quad (12)$$

In all cases above, the momentum fraction y of the quark within the photon is given by $y = M^2/(xs)$ and $f_{\gamma/e}(x)$ is the backscattered laser photon spectrum. The negative sign in front of the vector LQ asymmetries is a standard result: it comes about from the annihilation of 2 objects with opposite helicity into a vector particle. Another comment should be made at this time. Up to now, we've assumed that the beams will be polarized perfectly. This is probably not a bad assumption for the photon beam, as the backscattered photon beam will carry the polarization of the incident laser beam, and it should be straightforward to polarize the laser to a very high degree. Electron beam polarizations of order 70% can be expected, and this will modify some of our arguments. First, even if the LQ couples only to a particular helicity of electron, the contamination of the e beam with the wrong helicity will contaminate the signal. The finite polarization of the electron beam (λ_{beam}) will dilute the observable asymmetries by a factor λ_{beam} . Some care will have to be taken to ensure that any LQ signal observed with polarized beams is real, that is **not** due to contamination of the beam.

Having estimates of event numbers from previous works, we now need to determine if the different asymmetries predicted can be statistically separated. Due to a complete lack of data on parton distribution functions within a polarized photon, we need to use some theoretical input on the shapes of the helicity difference distribution functions of partons within the photon. There exist some parameterizations of the *asymptotic* polarized photon distribution functions [11,12], where it is assumed that Q^2 and x are large enough that the

Vector Meson Dominance part of the photon structure is not important, but rather the behavior is dominated by the point-like $\gamma q\bar{q}$ coupling. In this sort of approximation, the distribution functions take the form:

$$\Delta f_{q/\gamma}(x, Q^2) = \frac{\alpha}{\pi} \ln \left(\frac{Q^2}{\Lambda^2} \right) \frac{1}{x} \Delta p(x) \quad (13)$$

where $\Delta p(x)$ is a polynomial. In order to be consistent, we will use a similar asymptotic parameterization for the unpolarized photon distribution functions as well [13], even though various sets of more correct photon distribution functions exist (*e.g.*, [14–17]). We will only use this asymptotic approximation in the unpolarized case only for the calculation of the asymmetry, where it is hoped that in taking a ratio of the asymptotic polarized to the asymptotic unpolarized photon distribution functions, the error introduced will be minimized; still, we suggest that our results be considered cautiously at least in the relatively small LQ mass region. We note that in the asymptotic approximation, the unpolarized photon distribution functions have (not unexpectedly) a similar form to the polarized photon distribution functions:

$$f_{q/\gamma}(x, Q^2) = \frac{\alpha}{\pi} \ln \left(\frac{Q^2}{\Lambda^2} \right) \frac{1}{x^{1.6}} p(x) \quad (14)$$

where $p(x)$ is another polynomial. Finally, in regards to the question of the polarized photon distribution functions, a more careful calculation of the helicity difference distributions does exist [18] which includes the effect of VMD. However the authors of Ref. [18] give parameterizations of the ratio of the helicity difference to the helicity sum distribution functions that are independent of Q^2 . These are reported to be valid for $10 \leq Q^2 \leq 100$ GeV 2 . Given the large mass of the LQs being considered, the Q^2 is much too high to use these parameterizations.

We find that the asymmetry A_{LL} depends only on the dimensionless variable M/\sqrt{s} , though the event numbers depend on M and \sqrt{s} separately. For all the following figures, a) corresponds to the results at a 500 GeV e^+e^- collider operating in $e\gamma$ mode and b) corresponds to a 1 TeV e^+e^- collider operating in $e\gamma$ mode. Throughout, we use an integrated

luminosity of $50 \text{ fb}^{-1}/\text{yr}$ and the unpolarized photon distributions of Glück, Reya and Vogt [16] to estimate the number of LQ events in a given LQ model. Also, unless noted otherwise, our results are for $\kappa_L = \kappa_R = 1$. The first step in determining the leptoquark couplings would be to use electron polarization to divide the leptoquarks into subsets that couple only to left handed electrons, right handed electrons, or to both. Once this is done the asymmetry can be used to distinguish between leptoquarks within these subsets. We show, in Figure 1, A_{LL} vs. M for the set of LQs which couple only to left-handed electrons, that is S_3 , U_3 , \tilde{V}_2 and \tilde{R}_2 in the notation of BRW. The asymmetries for the vector LQs (U_3 and \tilde{V}_2) have been multiplied by -1 in order to reduce the scale to the point that the structure in the asymmetries is visible. That is, the scalar LQ's have positive values for A_{LL} while the vector LQ's have negative values for A_{LL} . In Figure 2, we show A_{LL} vs. M for the set of LQs which couple only to right-handed electrons, that is \tilde{S}_1 and \tilde{U}_1 . We again multiply the vector LQ (\tilde{U}_1) asymmetry by -1 . Finally, in Figures 3, 4 and 5 we show A_{LL} vs. M for the set of LQs which couple to both helicities of electrons, that is S_1 , V_2 , U_1 and R_2 . We again multiply the asymmetries of the vector LQs (V_2 and U_1) by -1 . As the asymmetries for this set of LQs depend on the arbitrary couplings κ_L and κ_R , we show results for various values of the κ s: in Figure 3, $\kappa_L = \kappa_R = 1$, in Figure 4, $\kappa_L = 1/2$ and $\kappa_R = 1$ and in Figure 5, $\kappa_L = 1$ and $\kappa_R = 1/2$.

Using earlier results, (*e.g.* Figure 3 of Ref. [7]), event numbers can be estimated and a statistical uncertainty in the measurement of A_{LL} (δA_{LL}) can also be estimated. For an asymmetry

$$A = \frac{\sigma(\alpha) - \sigma(\beta)}{\sigma(\alpha) + \sigma(\beta)} \quad (15)$$

the statistical uncertainty, δA_{LL} is given by the expression

$$\delta A_{LL} = \frac{1 - A^2}{\sqrt{1 - A}} \frac{1}{\sqrt{2N(\alpha)}} = \sqrt{\frac{1 - A^2}{N_{TOT}}} \quad (16)$$

where $N(\alpha)$ and N_{TOT} are $L\sigma(\alpha)$ and $L(\sigma(\alpha) + \sigma(\beta))$ respectively, with L being the integrated luminosity. These estimated δA_{LL} are shown in the error bars on Figures 1—5. It

can be seen that it is quite easy to distinguish a vector LQ from a scalar LQ, as A_{LL} is large and positive for all the scalar LQs while it is large and negative for vector LQs. For a LQ which couples only to left-handed electrons (see Figure 1), it will be possible to differentiate between the two possible vector or scalar LQs essentially up to the kinematical limit (remembering that the backscattered laser photon spectrum cuts off at an x of about 0.83; thus the maximum energy of an $e\gamma$ collider is slightly lower than the energy of the corresponding e^+e^- collider). If the LQ couples only to right-handed electrons (see Figure 2), there is only one vector and one scalar LQ possible, so it will be possible to determine the particular LQ essentially up to the kinematical limit. Finally, for a LQ which couples to both helicity electrons (see Figures 3, 4 and 5), it will be possible to differentiate between the two possible vector or scalar LQs essentially up to the kinematical limit, except for a small region of LQ mass where the asymmetries for the two types of scalar LQ are equal. The precise mass at which the crossover occurs depends on the values of $\kappa_{L,R}$. The limits quoted here assume a fully polarized electron beam; finite polarization will reduce these limits somewhat.

In conclusion, it certainly appears that a polarized $e\gamma$ collider can be used to differentiate between the different models of LQs that can exist, essentially up to the kinematic limit of the $e\gamma$ collider. Furthermore, it is quite straightforward to distinguish scalar LQs from vector LQs for all LQ mass (given that the LQ is kinematically allowed) with only a polarized electron beam. It is thus clear that a more careful analysis is warranted, with the following improvements:

- We rely on theoretical input for information on the parton distribution functions within a polarized photon; given the EMC (proton) spin crisis, there may be some surprises in the polarized photon as well.
- There are many questions as to the reliability of the asymptotic approximation to the photon distribution functions: are the values of y (the momentum fraction of the quark within the photon) and Q^2 large enough that the photon behaves asymptotically? Is it possible, at the very least (in the absence of experimental data) to improve

the theoretical input into the polarized photon distribution functions?

ACKNOWLEDGMENTS

This research was supported in part by the Natural Sciences and Engineering Research Council of Canada. The authors are grateful to Manuel Drees and Drew Peterson for helpful communications, to JoAnne Hewett for suggesting this particular analysis and to Tom Rizzo for continual encouragement.

REFERENCES

- [1] W. Buchmüller, R. Rückl, and D. Wyler, Phys. Lett. **B191**, 442 (1987).
- [2] H. Nadeau and D. London, Phys. Rev. **D47**, 3742 (1993).
- [3] J.L. Hewett and S. Pakvasa, Phys. Lett. **B227**, 178 (1989).
- [4] G. Bélanger, D. London and H. Nadeau, Université de Montréal preprint, (1993, unpublished).
- [5] J. E. Cieza Montalvo and O.J.P. Éboli, Phys. Rev. **D47**, 837 (1993).
- [6] O.J. Éboli, E.M. Gregores, M.B. Magro, P.G. Mercadante, and S.F. Novaes, Phys. Lett. **B311**, 147 (1993).
- [7] M.A. Doncheski and S. Godfrey, Phys. Rev. **D49**, 6220 (1994).
- [8] T.M. Aliev and Kh.A. Mustafaev, Yad. Fiz. **58**, 771 (1991).
- [9] M. Drees and R.M. Godbole, University of Wisconsin report MAD/PH/776 to appear in the proceedings of the Linear Collider Workshop, Waikoloa Hawaii, April 1993; M. Drees, M. Krämer, J. Zunft, and P.M. Zerwas, Phys. Lett. **B306**, 371 (1993); O.J.P. Éboli, M.C. Gonzalez-Garcia, F. Halzen, and S.F. Novaes, Phys. Lett. **B301**, 115 (1993); A.C. Bawa and W.J. Stirling, Z. Phys. **C57**, 165 (1993); M. Glück, E. Reya, and A. Weber, Phys. Lett. **B298**, 176 (1993); P. Chen, T.L. Barklow and M.E. Peskin, SLAC report SLAC 5873 (1993; unpublished); K.J. Abraham, Phys. Lett. **B316**, 365 (1993); E. Laenen, S. Riemersma, J. Smith and W. L. van Neerven, preprint ITP-SB-93-46 and hep-ph bulletin board # 9308295 (1993, unpublished).
- [10] CELLO Collaboration (H.-J. Behrend, *et al.*), Phys. Lett. **126B**, 391 (1983); PLUTO Collaboration (Ch. Berger, *et al.*), Phys. Lett. **142B**, 111 (1984); Nucl. Phys. **B281**, 365 (1987); JADE Collaboration (W. Bartel, *et al.*), Z. Phys. **C24**, 231 (1984); TASSO Collaboration (M. Althoff, *et al.*), Z. Phys. **C31** 527 (1986); TPC/Two-Gamma Col-

laboration (H. Aihara, *et al.*), Phys. Rev. Lett. **58**, 97 (1987); Z. Phys. **C34**, 1 (1987); AMY Collaboration (T. Sasaki, *et al.*), Phys. Lett. **B252**, 491(1990); H1 Collaboration (I. Abt, *et al.*), Phys. Lett. **B314**, 436(1993); OPAL Collaboration (R. Akers, *et al.*), CERN-PPE/93-156 (1993, unpublished).

- [11] J.A. Hassan and D.J. Pilling, Nucl. Phys. **B187**, 563 (1981).
- [12] Z. Xu, Phys. Rev. **D30**, 1440 (1984).
- [13] A. Nicolaidis, Nucl. Phys. **B163**, 156 (1980).
- [14] D.W. Duke and J.F. Owens, Phys. Rev. **D26**, 1600 (1982).
- [15] M. Drees and K. Grassie, Z. Phys. **C28**, 451 (1985); M. Drees and R. Godbole, Nucl. Phys. **B339**, 355 (1990).
- [16] M. Glück, E. Reya and A. Vogt, Phys. Lett. **B222**, 149 (1989); Phys. Rev. **D45**, 3986 (1992); Phys. Rev. **D46**, 1973 (1992).
- [17] H. Abramowicz, K. Charchula, and A. Levy, Phys. Lett. **B269**, 458 (1991).
- [18] M. Glück and W. Vogelsang, Z. Phys. **C57**, 309 (1993).

FIGURES

FIG. 1. A_{LL} vs. M for LQs which couple only to left-handed electrons; a) is for a 500 GeV collider and b) is for a 1 TeV collider. The solid curve is for an S_3 LQ, the dashed line is for a \tilde{V}_2 LQ ($-A_{LL}$ shown), the dotted line is for a U_3 LQ ($-A_{LL}$ shown) and the dotdashed line is for a \tilde{R}_2 LQ.

FIG. 2. A_{LL} vs. M for LQs which couple only to right-handed electrons; a) is for a 500 GeV collider and b) is for a 1 TeV collider. The solid curve is for an \tilde{S}_1 LQ and the dashed line is for a \tilde{U}_1 LQ ($-A_{LL}$ shown).

FIG. 3. A_{LL} vs. M for LQs which couple only to both left- and right-handed electrons; a) is for a 500 GeV collider and b) is for a 1 TeV collider; here $\kappa_L = \kappa_R = 1$. The solid curve is for an S_1 LQ, the dashed line is for a V_2 LQ ($-A_{LL}$ shown), the dotted line is for a U_1 LQ ($-A_{LL}$ shown) and the dotdashed line is for a R_2 LQ.

FIG. 4. A_{LL} vs. M for LQs which couple only to both left- and right-handed electrons; a) is for a 500 GeV collider and b) is for a 1 TeV collider; here $\kappa_L = 0.5$ and $\kappa_R = 1$. The solid curve is for an S_1 LQ, the dashed line is for a V_2 LQ ($-A_{LL}$ shown), the dotted line is for a U_1 LQ ($-A_{LL}$ shown) and the dotdashed line is for a R_2 LQ.

FIG. 5. A_{LL} vs. M for LQs which couple only to both left- and right-handed electrons; a) is for a 500 GeV collider and b) is for a 1 TeV collider; here $\kappa_L = 1$ and $\kappa_R = 0.5$. The solid curve is for an S_1 LQ, the dashed line is for a V_2 LQ ($-A_{LL}$ shown), the dotted line is for a U_1 LQ ($-A_{LL}$ shown) and the dotdashed line is for a R_2 LQ.

This figure "fig1-1.png" is available in "png" format from:

<http://arxiv.org/ps/hep-ph/9407317v1>

This figure "fig1-2.png" is available in "png" format from:

<http://arxiv.org/ps/hep-ph/9407317v1>

This figure "fig1-3.png" is available in "png" format from:

<http://arxiv.org/ps/hep-ph/9407317v1>

This figure "fig1-4.png" is available in "png" format from:

<http://arxiv.org/ps/hep-ph/9407317v1>

This figure "fig1-5.png" is available in "png" format from:

<http://arxiv.org/ps/hep-ph/9407317v1>

This figure "fig1-6.png" is available in "png" format from:

<http://arxiv.org/ps/hep-ph/9407317v1>

This figure "fig1-7.png" is available in "png" format from:

<http://arxiv.org/ps/hep-ph/9407317v1>

This figure "fig1-8.png" is available in "png" format from:

<http://arxiv.org/ps/hep-ph/9407317v1>

This figure "fig1-9.png" is available in "png" format from:

<http://arxiv.org/ps/hep-ph/9407317v1>

This figure "fig1-10.png" is available in "png" format from:

<http://arxiv.org/ps/hep-ph/9407317v1>

Figure 1a

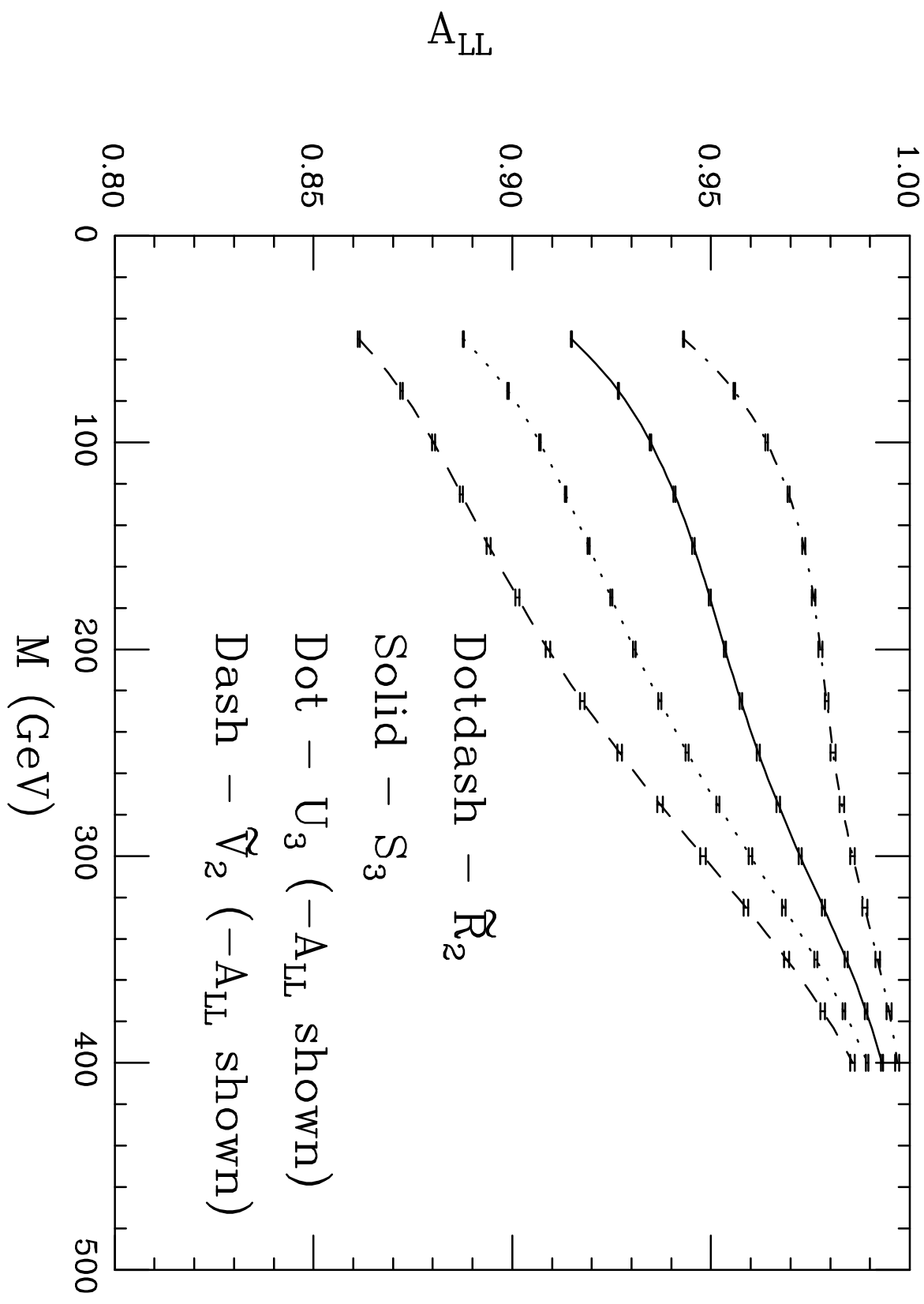


Figure 1b

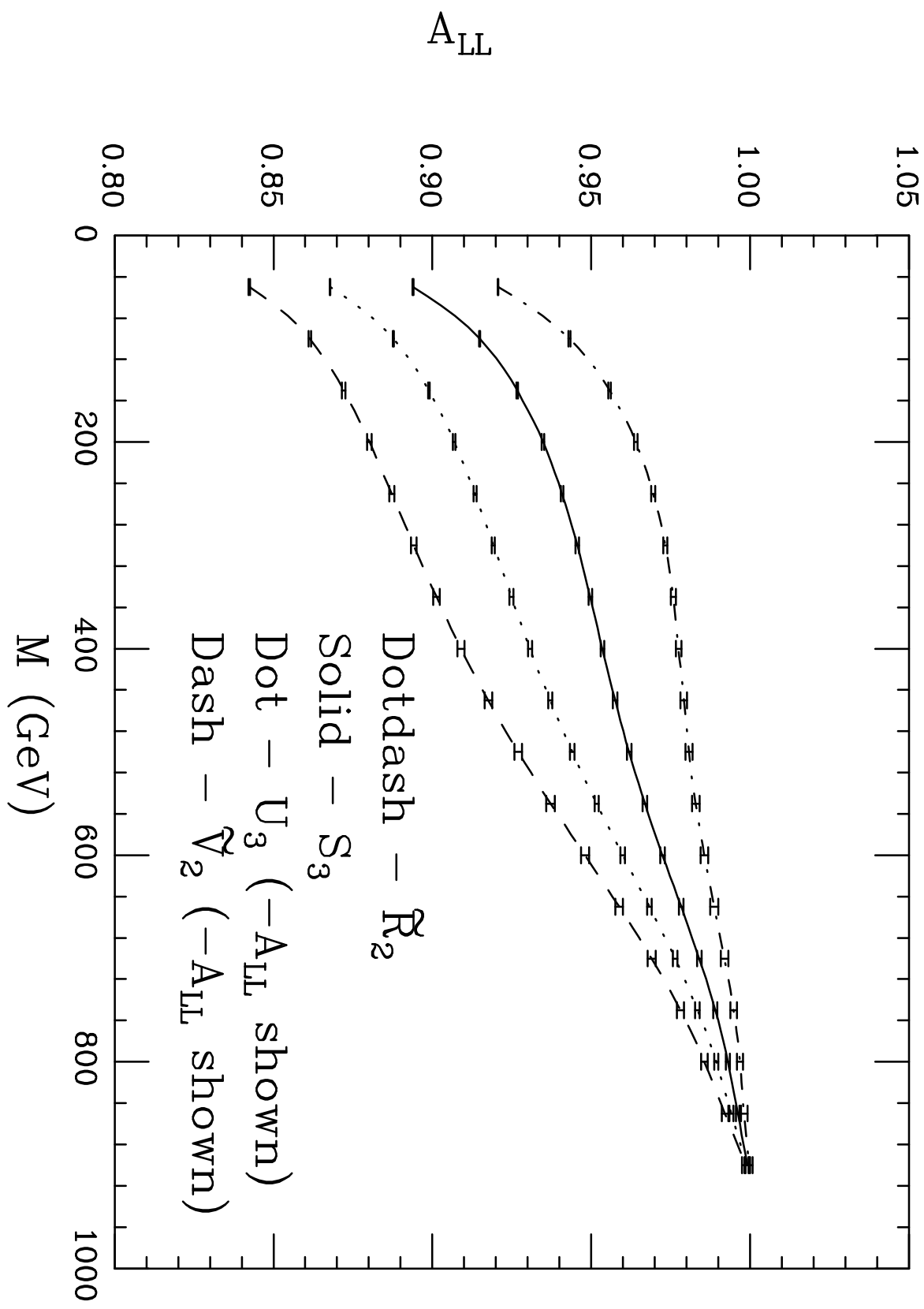


Figure 2a

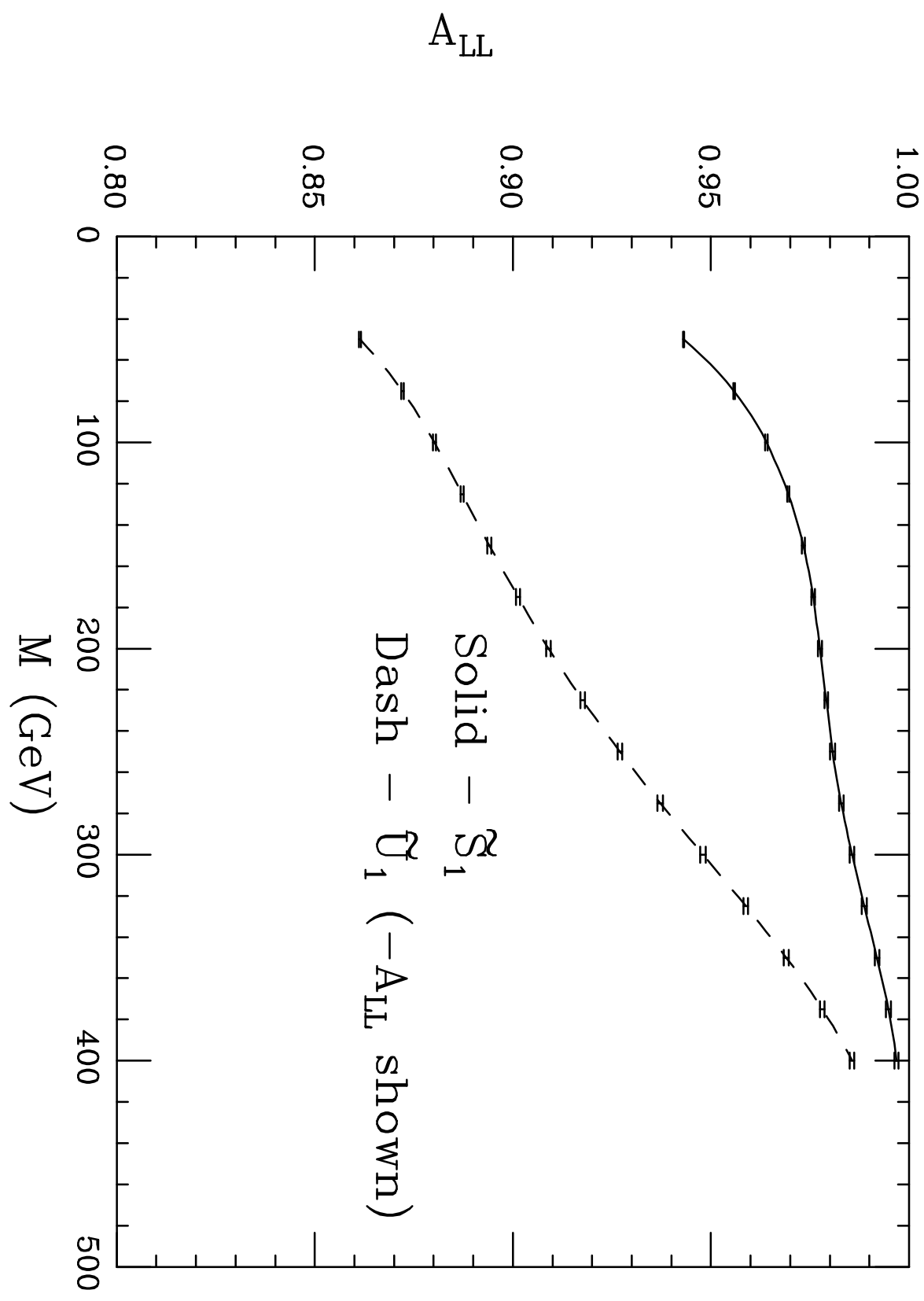


Figure 2b

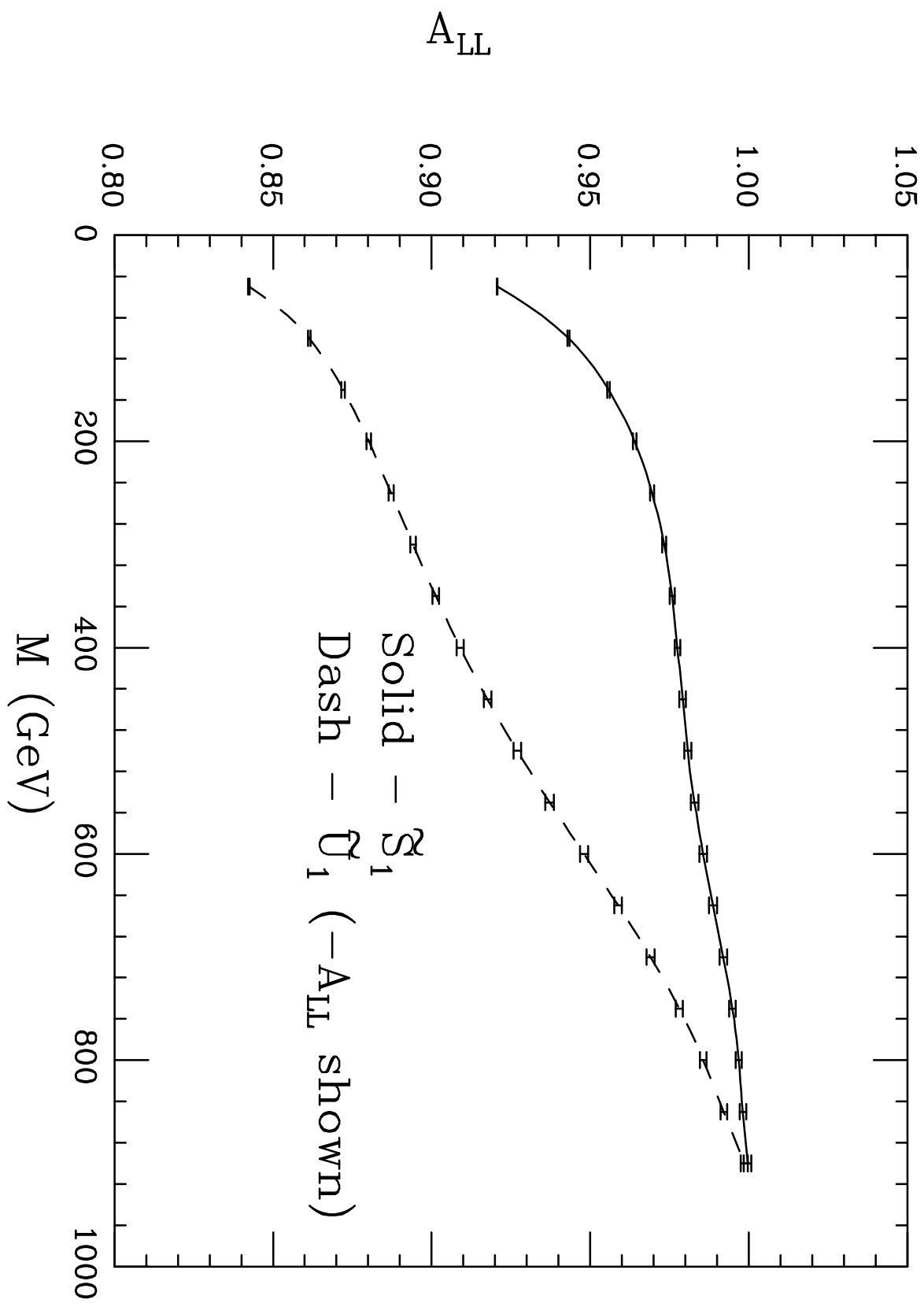


Figure 3a

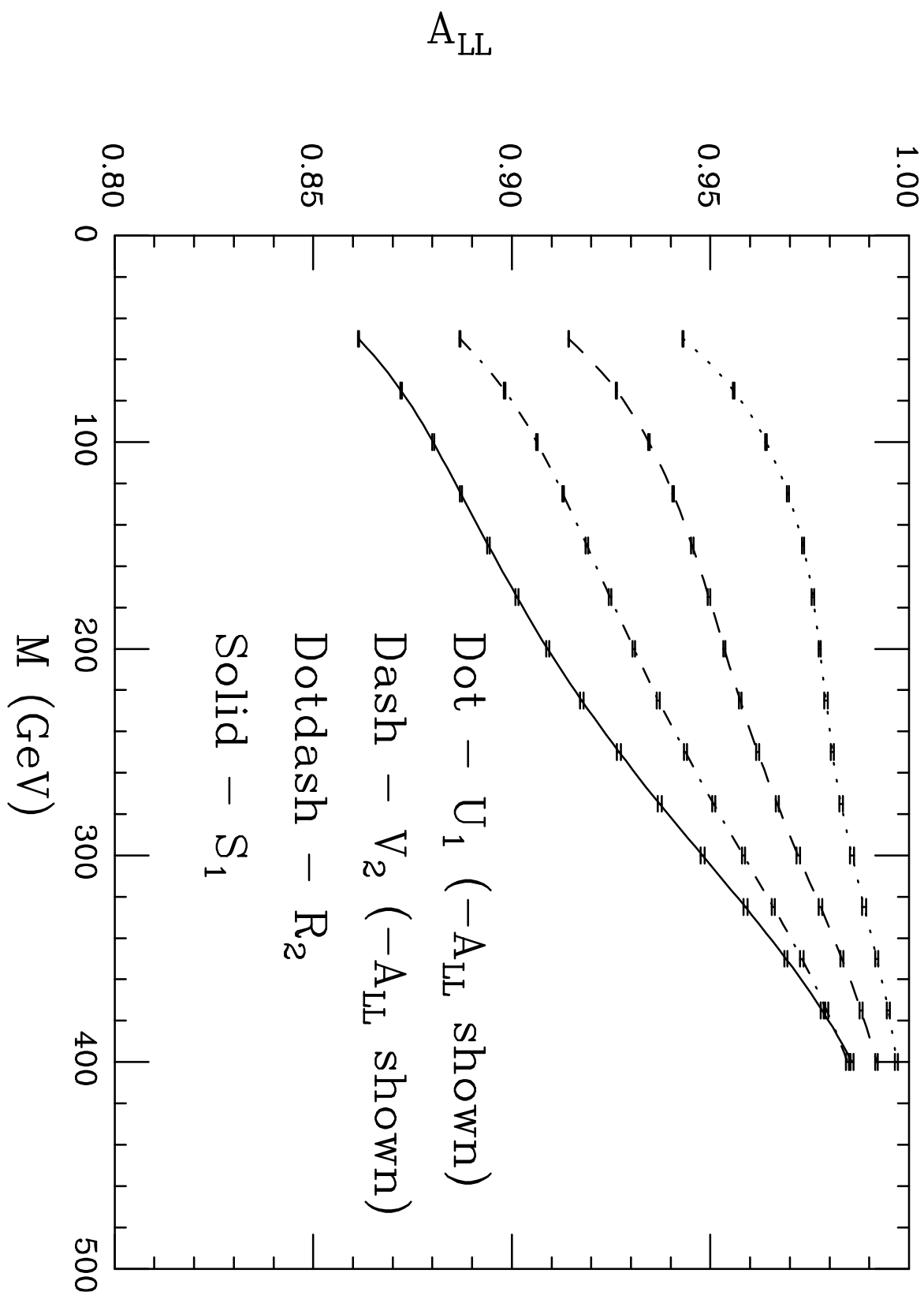


Figure 3b

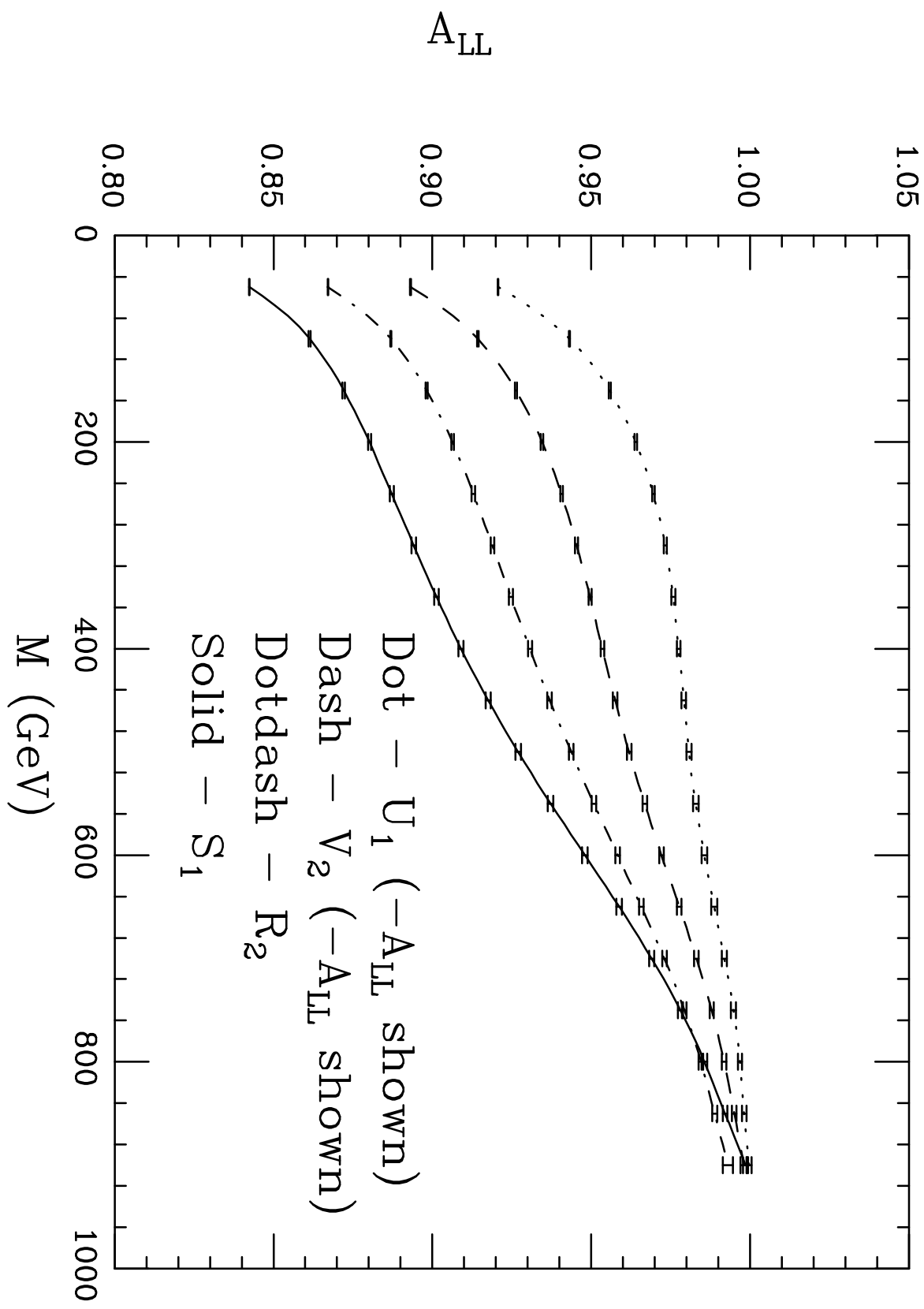


Figure 4a

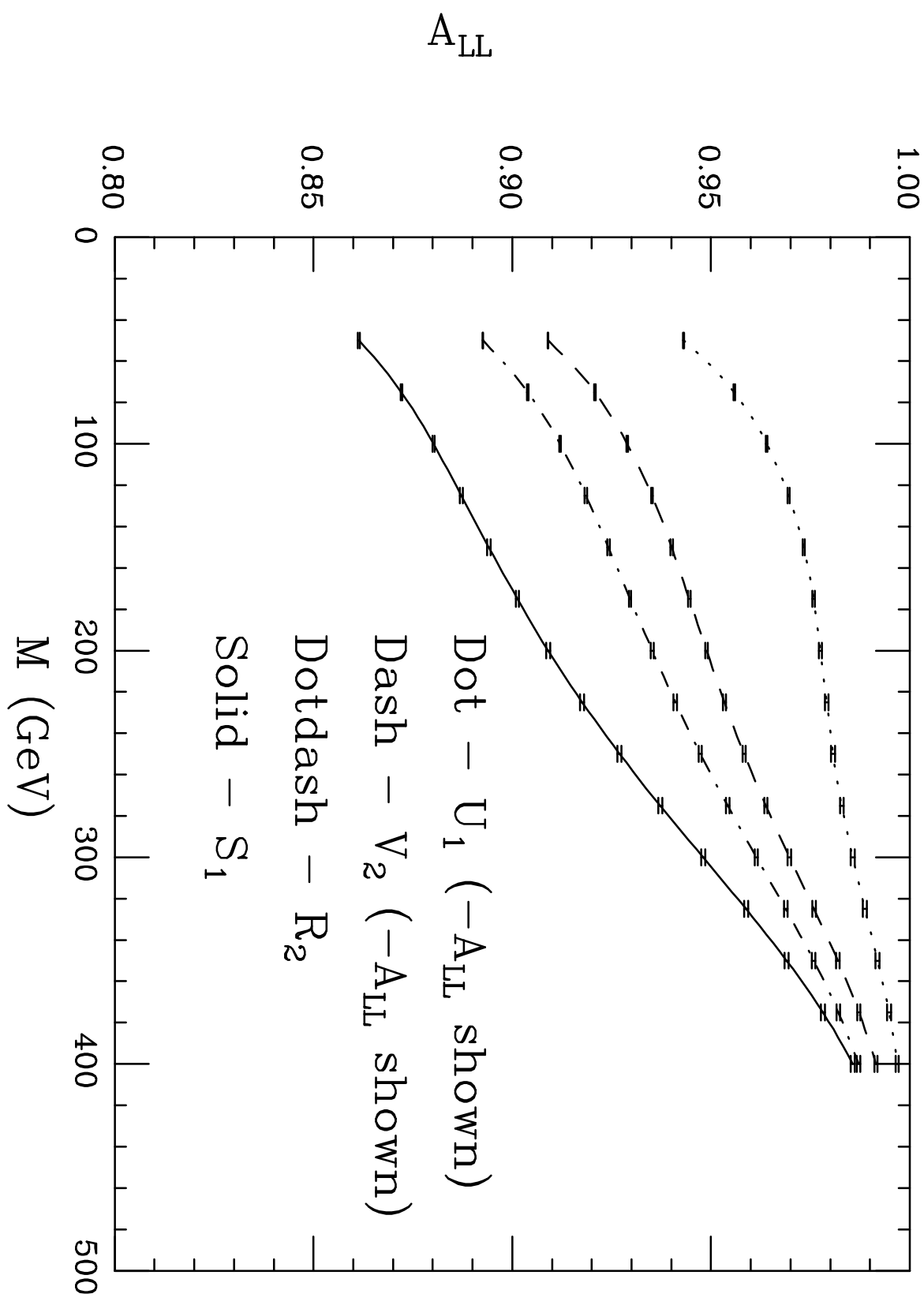


Figure 4b

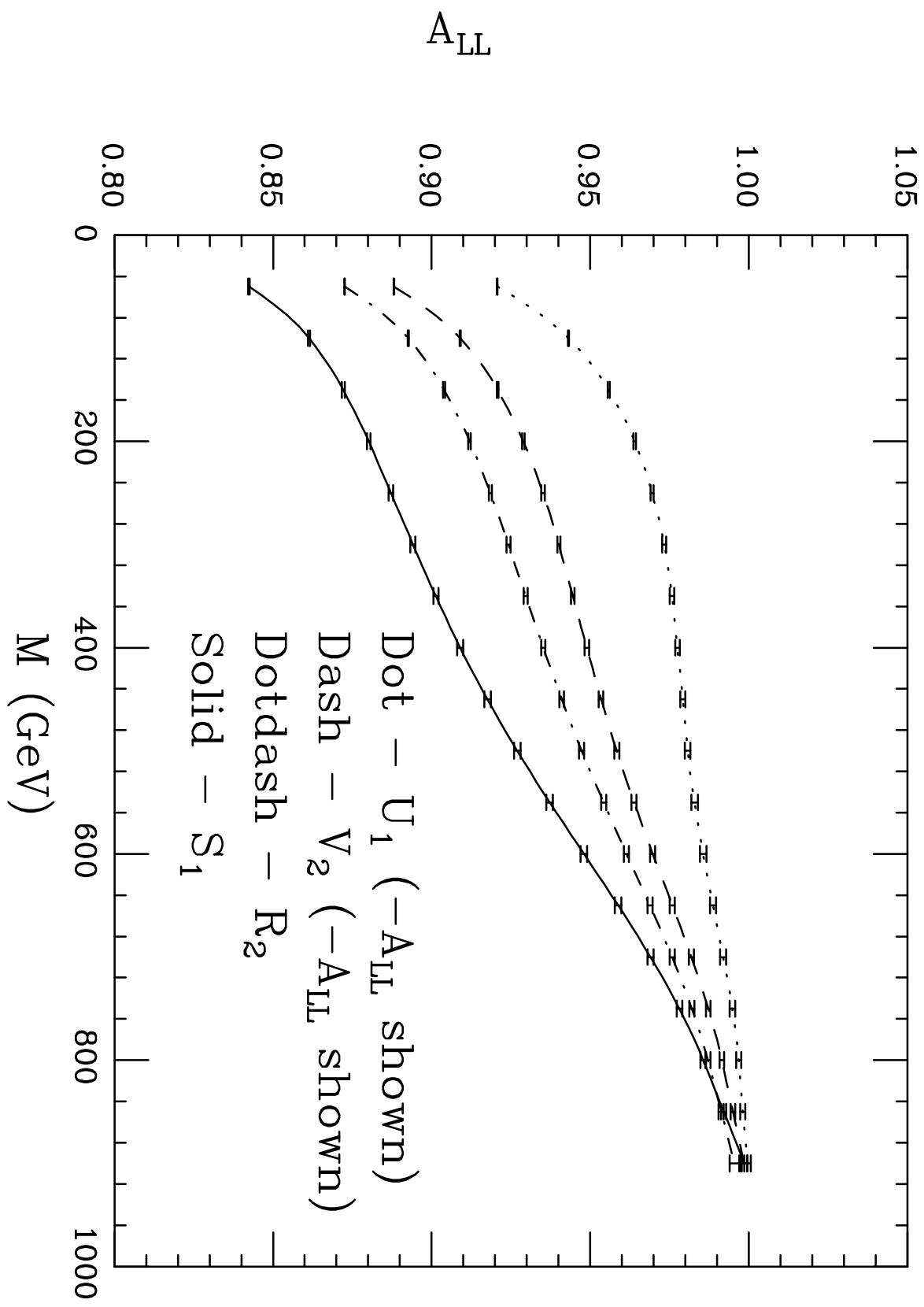


Figure 5a

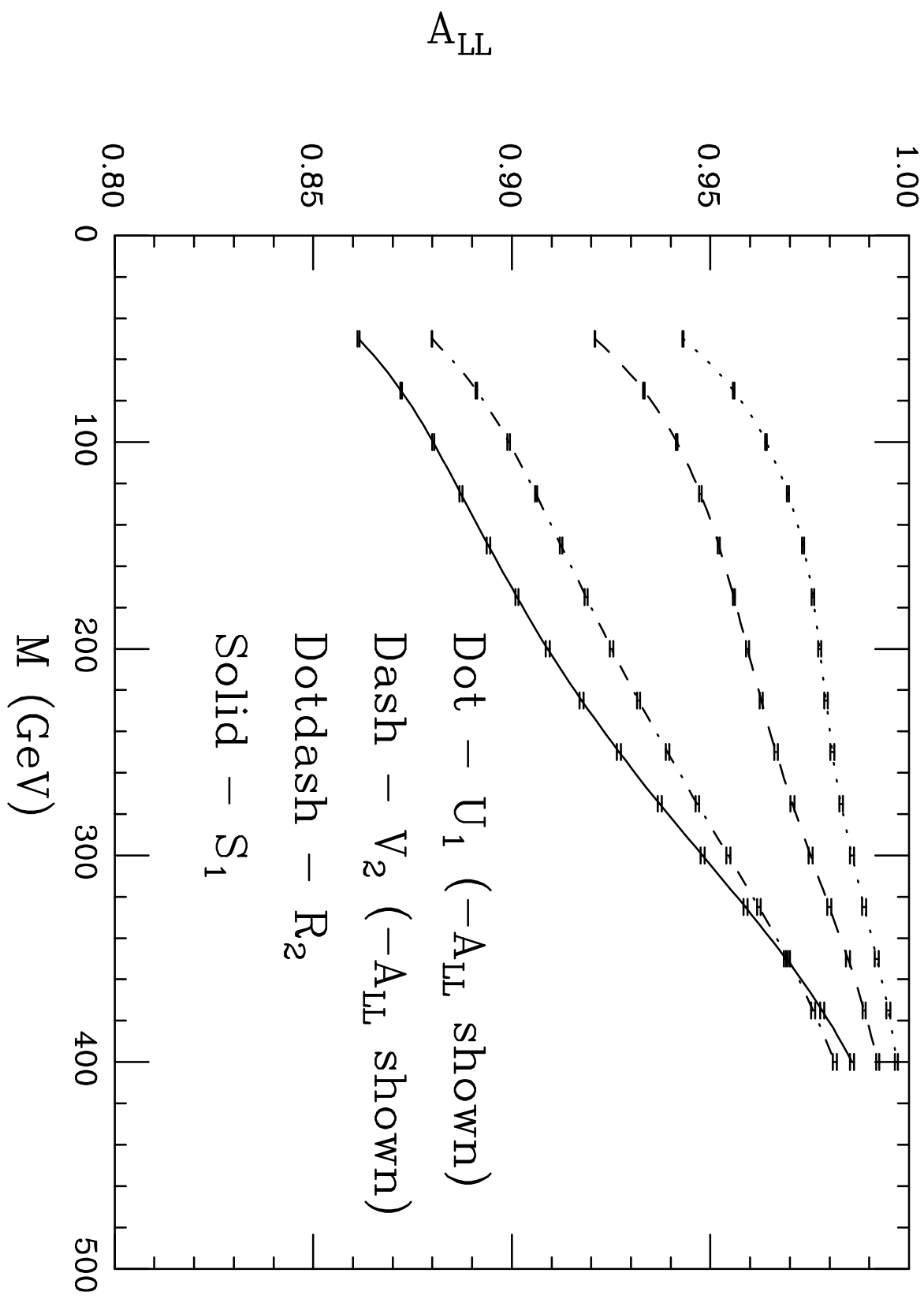


Figure 5b

